Aparici-Robles, F.; Davidhi, A.; Carot Sierra, JM.; Perez-Girbes, A.; Carreres-Polo, J.; Mazón-Momparler, M.; Juan-Albarracín, J.... (2022). Glioblastoma versus solitary brain metastasis: MRI differentiation using the edema perfusion gradient. Journal of Neuroimaging. 32(1):127-133. https://doi.org/10.1111/jon.12920

Received: 29 April 2021 | Revised: 18 July 2021 | Accepted: 5 August 2021

DOI: 10.1111/jon.12920

JOURNAL OF NEUROIMAGING
THE OFFICIAL JOURNAL OF THE AMERICAN SOCIETY OF NEUROIMAGING
WILEY

CLINICAL INVESTIGATIVE STUDY

# Glioblastoma versus solitary brain metastasis: MRI differentiation using the edema perfusion gradient

Fernando Aparici-Robles[1] | Andjoli Davidhi[1] | José Miguel Carot-Sierra[2] | Alexandre Perez-Girbes[1] | Joan Carreres-Polo[1] | Miguel Mazon Momparler[1] | Javier Juan - Albarracín[2] | Elies Fuster-Garcia[2] | Juan Miguel Garcia-Gomez[2]

[1] Servicio de Radiología, Área Clínica de Imagen Médica, Hospital Universitario y Politécnico La Fe, Valencia, Spain

[2] Instituto de Aplicaciones de las Tecnologías de la Información y de las Comunicaciones Avanzadas (ITACA), Universitat Politècnica de València, Valencia, Spain

**Correspondence**
Andjoli Davidhi, Servicio de Radiología, Área Clínica de Imagen Médica, Hospital Universitario y Politécnico La Fe, Avinguda de Fernando Abril Martorell, 106, Valencia 46026, Spain.
Email: davidhi-andy@hotmail.com

**Funding information**
This study was partially funded by SERAM (Spanish Society of Medical Radiology) Grant Becas Seram-Industria 2014.

## ABSTRACT

**Background and Purpose:** Differentiation between glioblastoma multiforme (GBM) and solitary brain metastasis (SBM) remains a challenge in neuroradiology with up to 40% of the cases to be incorrectly classified using only conventional MRI. The inclusion of perfusion MRI parameters provides characteristic features that could support the distinction of these pathological entities. On these grounds, we aim to use a perfusion gradient in the peritumoral edema.

**Methods:** Twenty-four patients with GBM or an SBM underwent conventional and perfusion MR imaging sequences before tumors' surgical resection. After postprocessing of the images, quantification of dynamic susceptibility contrast (DSC) perfusion parameters was made. Three concentric areas around the tumor were defined in each case. The monocompartimental and pharmacokinetics parameters of perfusion MRI were analyzed in both series.

**Results:** DSC perfusion MRI models can provide useful information for the differentiation between GBM and SBM. It can be observed that most of the perfusion MR parameters (relative cerebral blood volume, relative cerebral blood flow, relative Ktrans, and relative volume fraction of the interstitial space) clearly show higher gradient for GBM than SBM. GBM also demonstrates higher heterogeneity in the peritumoral edema and most of the perfusion parameters demonstrate higher gradients in the area closest to the enhancing tumor.

**Conclusion:** Our results show that there is a difference in the perfusion parameters of the edema between GBM and SBM demonstrating a vascularization gradient. This could help not only for the diagnosis, but also for planning surgical or radiotherapy treatments delineating the real extension of the tumor.

KEYWORDS
differentiation, glioblastoma, metastasis, MRI, perfusion gradient

## INTRODUCTION

Brain metastases are the most frequent brain tumors in adults, and up to 20–40% of cancer patients will develop them throughout their illness.[1] Most brain metastases originate from lung, breast, or melanoma malignancies, and approximately 50% of patients with metastatic brain disease present with solitary brain metastasis (SBM).[2,3] On the other hand, glioblastoma multiforme (GBM) is the

  

most common primary malignant neoplasm of Central Nervous System (CNS), accounting for half of them and the one with the worst prognosis.[4]

Differentiation between GBM and SBM is still one of the challenges in neuroradiology. Classically, some imaging features like location in the gray–white matter junction, noninfiltrating appearance, and previous malignancy help distinguish SBM from GBM.[3] However, conventional MRI alone classifies incorrectly up to 40% of the cases.[5] The inclusion of perfusion MRI information provides discriminating features that could support the differentiation between the aforementioned pathologies.[6–8]

Although both types of lesions show a perilesional hyperintensity on T2-WI corresponding to peritumoral edema, the edema of SBM is of vasogenic origin, whereas GBM edema is infiltrative and contains tumor cells and abnormal vascularization.[9] On these grounds, Lemercier et al.[5] defined the concept of apparent diffusion coefficient gradient in peritumoral edema of GBM. In their work, they confirm that there are differences in the diffusivity between the edema of the region closest to the tumor and the edema closest to the normal white matter.

Following the idea of peritumoral gradients, we hypothesize that there will be also a perfusion gradient in the GBM edema and it will be higher than the SBM edema.

## METHODS

The institutional review board approved this single-center retrospective study with data acquired between January 2014 and September 2016.

### Subjects

MRI examinations of 13 patients with pathologically proven SBM and 11 with GBM were obtained from our medical records to conduct this study. All patients were imaged, treated, and followed in our institution. All tumor diagnoses had been histologically verified according to the 2016 World Health Organization classification of CNS tumors.

### MRI image acquisition and data processing

All MRI scans were performed with our institution solitary brain lesion protocol with either 1.5T or a 3T (Signa HDxt 1.5 or 3 T, GE Healthcare, Waukesha, WI, USA) MRI system with a standard head coil. The brain MR protocol includes sagittal T1-weighted images, axial T2-weighted images, coronal fluid-attenuated inversion recovery (FLAIR) images, axial T2*-weighted gradient-recalled echo images, axial DW images, axial contrast-enhanced 3D T1-weighted images, and axial dynamic susceptibility contrast T2*-weighted gradient-echo perfusion images (DSC-PWI). The DSC-PWI sequence study was performed during the injection of gadolinium-based contrast agent (Multihance, Bracco, Italy). A bolus injection of 0.1 mmol/kg contrast agent was administered at 5 ml/s using a power injector (no prebolus administration). Saline was administered after the bolus injection. The study was acquired with the following parameters: 2000/25 ms Repetition Time/Echo Time; 128×128 matrix (1.8×1.8 mm in-plane resolution); 7 mm slice thickness; 60° flip angle; 14 cm full coverage cranio-caudal (20 slices); and 40 sequential temporally equidistant volumes each one with an acquisition time of 2 s. The baseline before injection of the bolus was five dynamics.

### Image processing

The study was performed according to four main steps: (1) MRI processing, (2) quantification of DSC perfusion, (3) definition of three concentric areas of the edema, and finally (4) the comparison of perfusion parameters at each concentric area.

The first step included the preprocessing of the morphologic images (pre and postgadolinium T1-weighted, T2-weighted, and FLAIR) and the DSC perfusion sequence. Regarding the morphologic images, we applied a noise reduction with adaptive nonlocal means[10] (search window of 7×7×7 pixels and patch window of 3×3×3 pixels), inhomogeneity correction with N4 algorithm[11] (100×100×100×0 iterations per scale), affine registration of all MR images to the postgadolinium T1 using ANTs software[12,13] (using mutual information metric and cubic Bsplines interpolation parameters), manual skull-stripping, and intensity normalization in the [0,255] range. As for DSC perfusion sequences, we applied the preprocessing algorithms of inhomogeneity correction with N4 (using a common bias field for all the images within the sequence), motion correction with ANTs software (considering rigid registration), registration of the first dynamic of the DSC sequence to the postgadolinium T1, and application of the transformation map to the rest of dynamics of the sequence, skull-stripping based on the mask defined for the morphological sequence, and temporal noise filtering using principal component analysis ensuring the 99% of variance and at least four components.

Second, concerning the DSC quantification, the arterial input function has been manually defined in the anterior cerebral artery of the unaffected contralateral hemisphere. The DSC quantification included both the monocompartmental[14] and the pharmacokinetic models.[15,16] As regards to the monocompartmental model, a correction of the extravasation was done using the Boxerman algorithm[17] and a nonlinear fitting of the concentration-time curves to a Gamma variate function. The monocompartmental quantification was based on the numeric integration of the Gamma corrected curves, while the quantification of the pharmacokinetic model was based on the nonlinear least squares fit to the Tofts standard model. All the quantification maps obtained were normalized to the unaffected contralateral white-matter tissue.

Third, we have analyzed the cerebral blood volume (CBV), cerebral blood flow (CBF), and mean transit time (MTT) from the

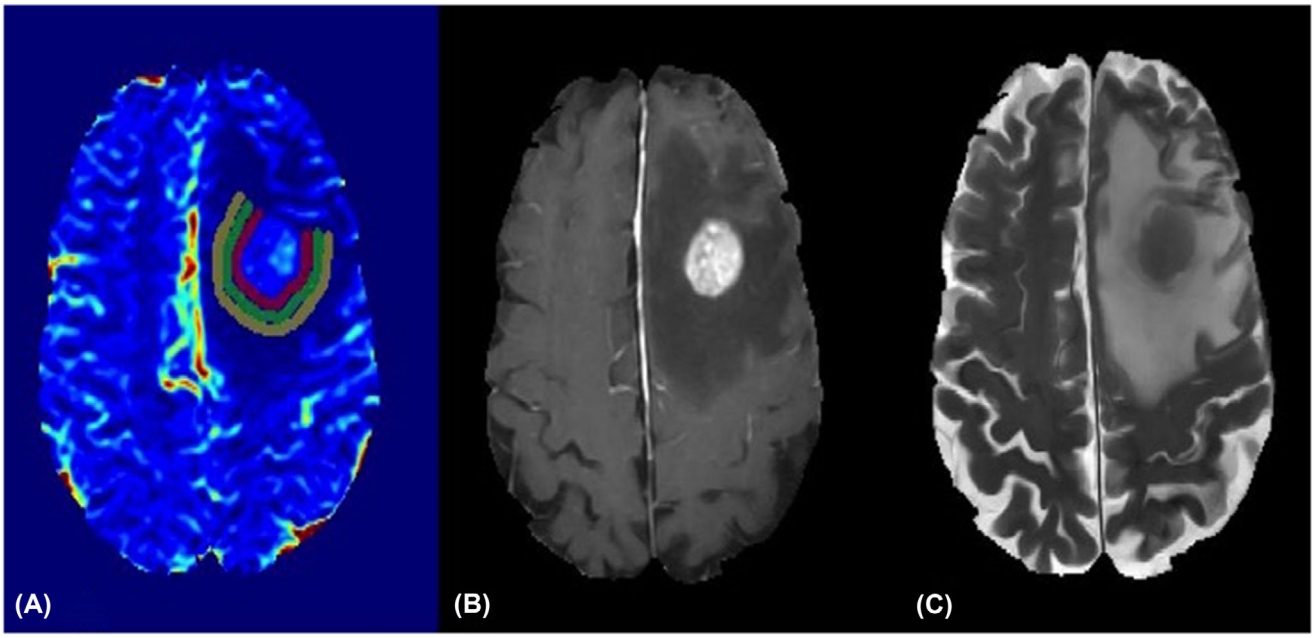


**FIGURE 1** Definition of the three regions of interest (ROIs) on the edema in a patient with solitary brain metastasis. (A) Postprocessing axial image of targeted temperature management with the concentric ROIs. (B) Fast spoiled gradient-echo enhanced Gd. (C) T2-weighted echo-planar imaging

monocompartmental model and the capillary permeability constant (Ktrans), the volume fraction of the interstitial space (ve), and the extraction coefficient or washing coefficient (Kep) from the pharmacokinetic model. All perfusion parameters have been normalized against the contralateral white matter not affected by the lesion.

Following the methodology used by Lemercier et al.,[5] different regions of interest (ROIs) in the edema area were manually marked out. As regards edema, it was defined as the region external to the tumor with uptake present in the fast spoiled gradient-echo sequence, hyperintensity pattern in the T2 sequence, and hypointensity shown in the CBV map. Three ROIs with approximate widths of 3 mm were delimited concentric and adjacent to the enhancing tumor (Figure 1). They were demarcated over the postgadolinium T1-weighted image, taking, also, into consideration the CBV map in order to avoid image registration problems. Hence, the ROIs were defined as:

- ROI1 (red) encompasses the peritumoral area of edema that is completely adjacent to the tumor
- ROI2 (green) represents a zone of edema at a distance of 3–6 mm from the viable tumor
- ROI3 (yellow) represents the region at a distance of 6–9 mm from the enhanced tumor and closely to white matter (Figure 2)

Once the ROIs were defined, the median and median absolute deviation (MAD) values of the perfusion parameters of each ROI's pixels were calculated. These values represent the vascularity of the patients' edema at different distances from the enhanced tumor. Median and MAD have been selected because they are robust statistics of the central tendency of the distributions.

## Statistical analysis

### Analysis of the differences in the three ROIs for the two types of tumors (GMB and SBM)

As the measurements in the three ROIs are from the same patient, an analysis of the differences was performed with a linear model with repeated measures. The between-subject factor is the type (GBM/SBM) and the within-subject factor is the ROI. According to the nature of the data, it is not necessary to resort to a nonparametric method. In order to determine which of the six observed variables best show the differences between the two types of metastasis and the three ROIs, a univariate approach has been used. Since sphericity cannot be assumed in all cases, the Greenhouse–Geisser correction has been used in repeated measures analysis. As the ROIs have the same distance, a test has been used to contrast the linearity or the quadratic effect of the distance on each of the six variables.

A classification model has been constructed using the discriminant analysis technique. The measurements of the six parameters in each of the three ROIs for each individual (18 variables in total per patient) have been used as variables in the discriminant analysis.

## RESULTS

The demographic data of the included patients are shown in Table 1.

It can be observed that most of the perfusion parameters (rCBV, rCBF, rKtrans, and rve) clearly demonstrate higher gradient for GBM

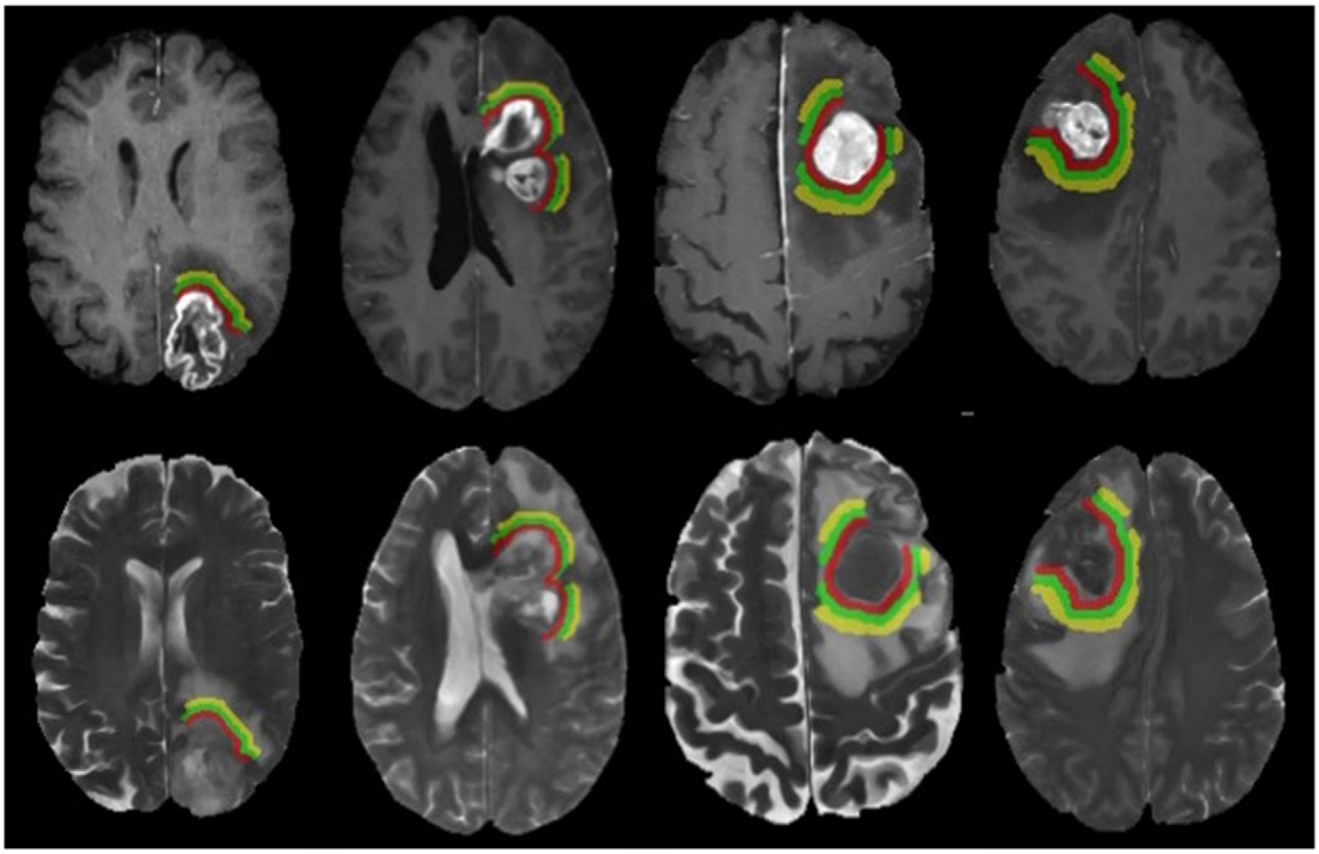

**FIGURE 2** Examples of the regions of interest (ROIs) defined for four different cases: RO1 (red) encompasses the peritumoral area of edema completely adjacent to the tumor. ROI2 (green) represents a zone of edema located from 3 to 6 mm from the viable tumor. ROI3 (yellow) represents the edema located from 6 to 9 mm area farthest from the enhanced tumor and close to the white matter

**TABLE 1** Demographic data of the included patients

| | GBM ($n = 13$) | SBM ($n = 11$) |
|---|---|---|
| Age, mean (IQR) years | 63.2 (14) | 61.5 (10) |
| Gender (F:M ratio) | 5:8 | 3:10 |
| Primary tumor, *n* (%) | | |
| Breast | – | 1 (7.7) |
| Colorectal | – | 3 (23.1) |
| Lung | – | 9 (69.2) |

Abbreviations: F, female; GBM, glioblastoma multiforme; IQR, interquartile range; M, male; *n*, number of patients; SBM, solitary brain metastasis.

than for SBM. This differentiation can be graphically observed in Figures 3 and 4 for monocompartimental and pharmacokinetic parameters, respectively. In other words, areas labeled ROI1 in GBM have higher levels of vascularity than areas labeled ROI2 or ROI3, whereas there are no substantial spatial variations in the peritumoral region in SBM cases.

The results of the statistics and *p*-values obtained for the type of tumor (GBM and SBM), the ROI, and the interaction between both factors are shown in Table 2.

In all variables, significant differences are observed in the levels measured in the three ROIs. The variables CBV, CBF, Ktrans, and rve have a similar behavior for each type of tumor, as there is an interaction between the ROI and the type of injury with this behavior: in GBM, there always are significantly higher, more pronounced values, and quadratic decrease with distance, while in SBM, significantly lower values and less decrease with distance are observed. In the rKep parameter, the differences between ROIs have the same tendency in the two types (no interaction is observed). On the other hand, MTT variable presents a different behavior from the rest of the variables: the differences between types are not significant, although they are significant for ROIs, although to a much lesser degree (without interaction between the two factors). In addition, the trend is increasing with distance and linear.

Classification using all variables shows a worse classification capacity than if you select variables using a stepwise process. In this process, only the variable rKep from ROI_1 remains as a variable in the discriminant function.

For this parameter, the ROC curve has been used to find a threshold to classify between GBM and SBM. The optimal point has been determined using Youden's criteria. The value obtained is rKep = 0.9628, which provides a sensitivity of 0.923 and a specificity of 0.8460, with an area under the curve of 0.876 (Figure 5).

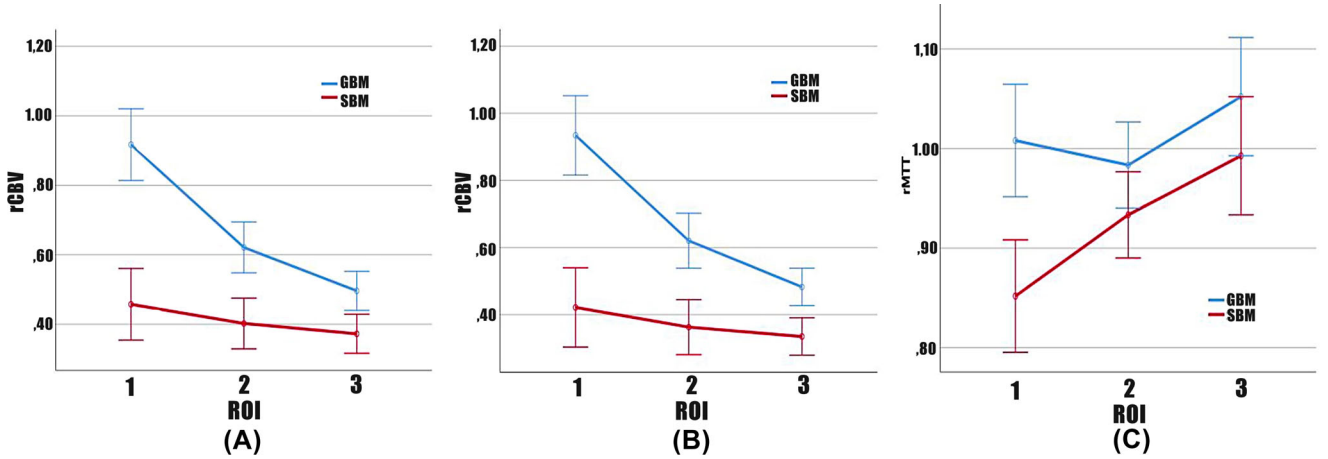


**FIGURE 3** Plot of the relative cerebral blood volume (rCBV) (A), relative cerebral blood flow (rCBF) (B), and relative mean transit time (rMTT) (C) perfusion values (median+/-mean absolute deviaton) in each region of interest (ROI), for solitary brain metastasis (SBM) (blue line) and glioblastoma (GBM) (red line)

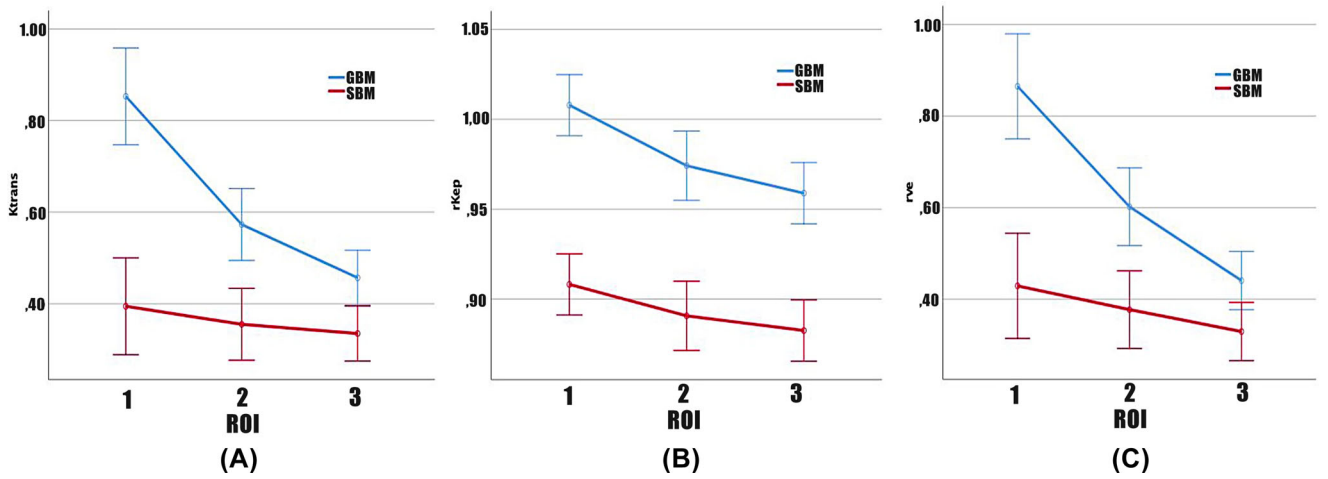


**FIGURE 4** Plot of the capillary permeability constant (Ktrans) (A), relative extraction coefficient (rKep) (B), and relative volume fraction of the interstitial space (rve) (C) perfusion values (median+/-mean absolute deviation) in each region of interest (ROI), for solitary brain metastasis (SBM) (blue line) and glioblastoma (GBM) (red line)

## DISCUSSION

In this study, we compared the perfusion gradient of GBM and SBM using a regional segmentation method and investigated the infiltration behavior of GBM as potential justification of our results.

Differentiation between GBM and SBM remains a challenge in neuroradiology with up to 40% of the cases to be incorrectly classified using only conventional MRI.[5] The inclusion of perfusion MRI parameters provides characteristic features that could support the distinction of these pathological entities. This differentiation between GBM and SBM has been previously studied by characterizing the lesions and the peritumoral edema. Specifically, differences in diffusion[5,18,19] and perfusion[20–23] of the edema have been previously observed. Regarding perfusion, Lehmann et al.[22] showed that perfusion parameters (e.g., rCBV) associated with morphological MR parameters can help in the differentiation of GBM from cerebral metastasis. As for the tumor itself, the efforts have been directed toward cerebral perfusion,[7,8,14,16] diffusion,[24,25] or their combination.[3]

It is well known that GBM tumor cells are not confined to the enhancing tumor and conventional MRI fails to delineate the whole tumor extension. This is because peritumoral edema also contains tumor cells and high vascularization due to tumor angiogenesis. Our results are consistent with other imaging papers in which other perfusion sequences are evaluated.[6–8,16] Specifically, Sunwoo et al.[7] showed that, using arterial spin labeling MRI, perfusion parameters, such as CBF, were significantly higher in the peritumoral region of GBM compared to brain metastasis ($p<0.001$) with an area under the curve of 0.835.

**TABLE 2** Effects of differences between GBM/SBM, between the three ROIs, and that of their interaction using the values of the six parameters studied for each ROI

| | | *F* | *p*-value |
|---|---|---|---|
| Type of tumor(GBM/SBM) | CBV | 6.285 | 0.019 |
| | CBF | 6.772 | 0.016 |
| | MTT | 1.729 | 0.201 |
| | KTrans | 5.626 | 0.026 |
| | rKep | 12.728 | 0.002 |
| | rve | 4.547 | 0.043 |
| ROI | CBV | 32.46 | 0.000 |
| | CBF | 24.98 | 0.000 |
| | MTT | 5.021 | 0.011 |
| | KTrans | 26.574 | 0.000 |
| | rKep | 21.28 | 0.000 |
| | rve | 26.95 | 0.000 |
| ROI x Type | CBV | 14.51 | 0.000 |
| | CBF | 11.52 | 0.000 |
| | MTT | 1.93 | 0.157 |
| | KTrans | 14.62 | 0.000 |
| | $rK_{ep}$ | 2.09 | 0.140 |
| | rve | 10.51 | 0.002 |

Abbreviations: CBF, cerebral blood flow; CBV, cerebral blood volume; GBM, glioblastoma multiforme; Ktrans, capillary permeability constant; MTT, mean transit time; rKep, relative extraction coefficient constant; ROI, region of interest; rve, relative volume fraction; SBM, solitary brain metastasis.

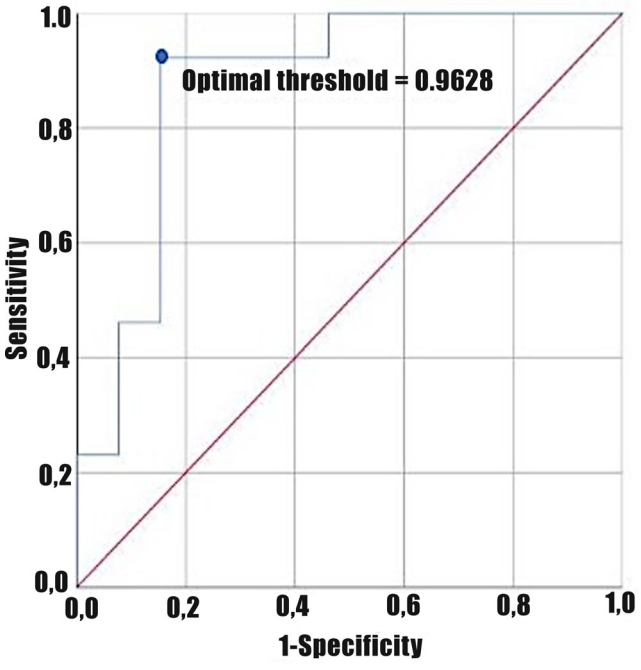


**FIGURE 5** Receiver operating characteristic curve and optimal threshold calculated with Youden J statistic for relative extraction coefficient

Regarding SBM, the perfusion parameters (except rKep and MTT) exhibit smaller gradients than GBM between its edema and the normal appearing white matter due to edema's vasogenic origin. However, GBM demonstrates higher heterogeneity in the peritumoral edema and most of the perfusion parameters (except rKep and MTT) show higher gradients in the area closest to the enhancing tumor. The concept of perfusion gradient in peritumoral edema has also been developed by Lin et al.[26] from a similar perspective. In their study, using Magnetic Resonance spin labeling, CBV and CBF present a gradient as we move away from GBM that does not exist in SBM. These data support our results. This behavior in GBM is expected due to the infiltration gradient observed in histological images of the tumor[9,27] and agrees with the results in previous studies indicating the existence of differences in GBM edema as a function of proximity to the lesion.

The vascular gradient also allows discrimination of patients with primary or metastatic GBM showing 96.28% of sensitivity and 15.40% of specificity. However, this finding is still limited by the number of cases and methodology used in this study.

This study confirms, with its limitations, that DSC perfusion MRI models can provide useful information not only for diagnosis, but also for planning surgical or radiotherapy treatments delineating the real extension of the tumor.

It is necessary to consider that the correct evaluation of the vascularity gradient requires assessing the gradient with respect to the remoteness from the tumor. That is, the width of each of the ROIs must consider the speed with which vascular enhancement gradually disappears to avoid the accumulation of the most part of the gradient in ROI1 and not its homogeneous distribution.

It is worth noticing that the delineation of the ROIs on edema was performed mainly on the T2* perfusion sequence, aided by the T2 sequence and the anatomic T1 sequence after administration of contrast agent. If the aforementioned ROIs had been defined solely on the anatomical T2 sequence, the errors of registration between the MR sequences would have easily masked the vascular behavior, due to the inclusion of gray matter, white matter, or cerebrospinal fluid in the regions.

DSC perfusion MRI models can provide useful information for the differentiation between GBM and SBM. GBM demonstrates higher heterogeneity in the peritumoral edema and most of the perfusion parameters demonstrate higher gradients in the area closest to the enhancing tumor. Our results show that there is a difference in the perfusion parameters of the edema between SBM and GBM demonstrating a vascularization gradient. This could help not only for the diagnosis, but also for planning surgical or radiotherapy treatments delineating the real extension of the tumor.

## ACKNOWLEDGMENTS AND DISCLOSURE

All procedures performed in studies involving human participants were in accordance with the ethical standards of the institutional and/or national research committee and with the 1964 Helsinki declaration and its later amendments or comparable ethical standards. The authors declare that they have no conflict of interest. Informed patient consent have been obtained.

## ORCID

*Andjoli Davidhi* https://orcid.org/0000-0002-5507-8644


## REFERENCES


1. Gavrilovic IT, Posner JB. Brain metastases: epidemiology and pathophysiology. J Neurooncol 2005;75:5-14.
2. Ranjan T, Abrey LE. Current management of metastatic brain disease. Neurother J Am Soc Exp Neurother 2009;6:598-603.
3. Bauer AH, Erly W, Moser FG, Maya M, Nael K. Differentiation of solitary brain metastasis from glioblastoma multiforme: a predictive multiparametric approach using combined MR diffusion and perfusion. Neuroradiology 2015;57:697-703.
4. Ohgaki H, Kleihues P. Epidemiology and etiology of gliomas. Acta Neuropathol 2005;109:93-108.
5. Lemercier P, Paz Maya S, Patrie JT, Flors L, Leiva-Salinas C. Gradient of apparent diffusion coefficient values in peritumoral edema helps in differentiation of glioblastoma from solitary metastatic lesions. AJR Am J Roentgenol 2014;203:163-9.
6. Jung BC, Arevalo-Perez J, Lyo JK, et al. Comparison of glioblastomas and brain metastases using dynamic contrast-enhanced perfusion MRI. J Neuroimaging 2016;26:240-6.
7. Sunwoo L, Yun TJ, You SH, et al. Differentiation of glioblastoma from brain metastasis: qualitative and quantitative analysis using arterial spin labeling MR imaging. PLoS One 2016;11:1-13.
8. Lu S, Gao Q, Yu J, et al. Utility of dynamic contrast-enhanced magnetic resonance imaging for differentiating glioblastoma, primary central nervous system lymphoma and brain metastatic tumor. Eur J Radiol 2016;85:1722-7.
9. Claes A, Idema AJ, Wesseling P. Diffuse glioma growth: a guerilla war. Acta Neuropathol 2007;114:443-58.
10. Manjón JV, Coupé P, Martí-Bonmatí L, Collins DL, Robles M. Adaptive non-local means denoising of MR images with spatially varying noise levels. J Magn Reson Imaging 2010;31:192-203.
11. Tustison NJ, Avants BB, Cook PA, et al. N4ITK: improved N3 bias correction. IEEE Trans Med Imaging 2010;29:1310-20.
12. Avants BB, Epstein CL, Grossman M, Gee JC. Symmetric diffeomorphic image registration with cross-correlation: evaluating automated labeling of elderly and neurodegenerative brain. Med Image Anal 2008;12:26-41.
13. Klein A, Andersson J, Ardekani BA, et al. Evaluation of 14 nonlinear deformation algorithms applied to human brain MRI registration. Neuroimage 2009;46:786-802.
14. Revert Ventura AJ, Sanz-Requena R, Martí-Bonmatí L, et al. [Nosological analysis of MRI tissue perfusion parameters obtained using the unicompartmental and pharmacokinetic models in cerebral glioblastomas]. Radiologia 2010;52:432-41.
15. Tofts PS, Kermode AG. Measurement of the blood–brain barrier permeability and leakage space using dynamic MR imaging. 1. Fundamental concepts. Magn Reson Med 1991;17:357-67.
16. Law M, Yang S, Babb JS, et al. Comparison of cerebral blood volume and vascular permeability from dynamic susceptibility contrast-enhanced perfusion MR imaging with glioma grade. AJNR Am J Neuroradiol 2004;25:746-55.
17. Boxerman JL, Schmainda KM, Weisskoff RM. Relative cerebral blood volume maps corrected for contrast agent extravasation significantly correlate with glioma tumor grade, whereas uncorrected maps do not. AJNR Am J Neuroradiol 2006;27:859-67.
18. Lee EJ, Ahn KJ, Lee EK, Lee YS, Kim DB. Potential role of advanced MRI techniques for the peritumoural region in differentiating glioblastoma multiforme and solitary metastatic lesions. Clin Radiol 2013;68:e689-e97.
19. Sparacia G, Gadde JA, Iaia A, Sparacia B, Midiri M. Usefulness of quantitative peritumoural perfusion and proton spectroscopic magnetic resonance imaging evaluation in differentiating brain gliomas from solitary brain metastases. Neuroradiol J 2016;29:160-7.
20. Blasel S, Jurcoane A, Franz K, Morawe G, Pellikan S, Hattingen E. Elevated peritumoural rCBV values as a mean to differentiate metastases from high-grade gliomas. Acta Neurochir (Wien) 2010;152:1893-9.
21. Halshtok Neiman O, Sadetzki S, Chetrit A, Raskin S, Yaniv G, Hoffmann C. Perfusion-weighted imaging of peritumoral edema can aid in the differential diagnosis of glioblastoma mulltiforme versus brain metastasis. Isr Med Assoc J 2013;15:103-5.
22. Lehmann P, Saliou G, De Marco G, et al. Cerebral peritumoral oedema study: does a single dynamic MR sequence assessing perfusion and permeability can help to differentiate glioblastoma from metastasis? Eur J Radiol 2012;81:522-7.
23. Abe T, Mizobuchi Y, Sako W, et al. Clinical significance of discrepancy between arterial spin labeling images and contrast-enhanced images in the diagnosis of brain tumors. Magn Reson Med Sci 2015;14:313-9.
24. Yang G, Jones TL, Barrick TR, Howe FA. Discrimination between glioblastoma multiforme and solitary metastasis using morphological features derived from the p:q tensor decomposition of diffusion tensor imaging. NMR Biomed 2014;27:1103-11.
25. Caravan I, Ciortea CA, Contis A, Lebovici A. Diagnostic value of apparent diffusion coefficient in differentiating between high-grade gliomas and brain metastases. Acta Radiol 2018;59:599-605.
26. Lin L, Xue Y, Duan Q, et al. The role of cerebral blood flow gradient in peritumoral edema for differentiation of glioblastomas from solitary metastatic lesions. Oncotarget 2016;7:69051-9.
27. Giese A, Bjerkvig R, Berens ME, Westphal M. Cost of migration: invasion of malignant gliomas and implications for treatment. J Clin Oncol 2003;21:1624-36.



**How to cite this article:** Aparici-Robles F, Davidhi A, Carot-Sierra JM, Perez-Girbes A, Carreres-Polo J, Momparler MM, et al. Glioblastoma versus solitary brain metastasis: MRI differentiation using the edema perfusion gradient. *J Neuroimaging*. 2021;1–7. https://doi.org/10.1111/jon.12920